Journal of Hydrology 578 (2019) 124071

Contents lists available at ScienceDirect

Journal of Hydrology

journal homepage: www.elsevier.com/locate/jhydrol

Research papers

Soil water freezing model with non-iterative energy balance accounting

Tomas Vogel*, Michal Dohnal, Jana Votrubova, Jaromir Dusek

Czech Technical University in Prague, Faculty of Civil Engineering, Prague, Czech Republic

ARTICLE INFO

This manuscript was handled by Corrado Corradini, Editor-in-Chief, with the assistance of Wei Hu, Associate Editor

Keywords:
Soil freezing
Energy balance equation
Phase transition
Equivalent liquid water content
Finite element method
Numerical simulations

ABSTRACT

A new modeling approach was developed to facilitate simulations of soil water flow and energy transport during sporadic freezing–thawing episodes typical for the winter regime of humid-temperate continental climate. The approach is based on an accurate non-iterative algorithm for solving the highly non-linear energy balance equation during phase transitions. The new algorithm was successfully verified against the analytical solution for idealized freezing and thawing conditions. Two examples of the model application – under hypothetical and real field conditions – are given.

1. Introduction

The physically sound description of processes accompanying phase transitions during freezing and thawing of soil water is a task that has received growing attention in the recent literature. The related studies focused on different aspects of the soil freezing phenomena, addressing the impact of phase transitions on the soil thermal budget (e.g. Luo et al., 2003), the snowmelt runoff enhancement by frozen soil conditions (e.g. Cherkauer and Lettenmaier, 1999), the permafrost fate modeling (e.g. Riseborough, et al., 2008), the frost heaving effects (e.g. Peppin and Style, 2013), etc.

In soils, pore water freezes over a relatively narrow range of temperatures below the freezing point of pure water (273.15 K at normal atmospheric pressure). The relationship between freezing point depression and liquid water saturation of a particular soil can be described by a soil freezing curve. Soil freezing curves can be determined experimentally, predicted based on the physics of liquid-ice interface or estimated using empirical expressions. The exact course of freezing curves is, however, difficult to determine with accuracy.

The shape of freezing curves is often predicted using the generalized Clausius-Clapeyron equation (Koopmans and Miller, 1966; Kay and Groenevelt, 1974; Spaans and Baker, 1996) or Gibbs-Thomson equation (e.g. Strange et al., 1993; Mitchell et al., 2008). These equations predict the freezing point depression of about one degree Celsius over the range of pore sizes from 1 mm to 0.1 μm. The adequacy of these two equations (leading to very similar predictive formulas) is based on several simplifying assumptions: (i) Thermodynamic equilibrium at the ice–liquid interface during phase transitions is assumed. (ii) The ice pressure is usually approximated by atmospheric pressure. (iii) The curvature of the ice–liquid interface is assumed to be similar to the liquid–air interface, invoking the freezing–drying analogy. Although these assumptions have been accepted as reasonable working hypotheses by most researchers, some aspects of the underlying theory have been disputed. For example: The thermodynamic equilibrium at the soil freezing front was questioned by Ma et al. (2015), arguing that soil freezing may tend to be a non-equilibrium (irreversible) thermodynamic process. Equating ice pressure with atmospheric pressure may be inappropriate in unsaturated soils where ice–air interface exists in addition to ice–liquid interface (e.g. Miller, 1980). The freezing-drying analogy assumption was criticized by Hohmann (1997), who pointed out to the physical dissimilarity of the two processes.

As pointed out e.g. by McKenzie et al. (2007), the shape of soil freezing curve is very important when apparent heat capacity concept (e.g. Harlan, 1973) is used to formulate energy balance equation in freezing soil models. The concept combines soil heat capacity with the slope of freezing curve. The slope is obtained by differentiating the soil freezing function, which is usually very steep, thus dominating the resulting value of apparent heat capacity coefficient during phase transitions. Uncertainties associated with the determination of freezing curves propagate through this coefficient to the energy balance equation – enhanced by the differentiation procedure, which in turn negatively affects the accuracy of model predictions.

There is a strong experimental evidence that processes occurring at the ice–liquid interface during freezing of soil water cause lowering of

* Corresponding author.
E-mail address: vogel@fsv.cvut.cz (T. Vogel).

https://doi.org/10.1016/j.jhydrol.2019.124071
Received 12 June 2019; Received in revised form 8 August 2019; Accepted 23 August 2019
Available online 24 August 2019
0022-1694/

soil water potential, which leads to the migration of water from unfrozen soil below freezing front toward the front — the phenomenon often referred to as cryosuction (Taber, 1930; Coussy, 2005; Peppin and Style, 2013; Kurylyk and Watanabe, 2013). Additional depression of freezing point temperature and soil water potential at the freezing front can be caused by the presence of solutes in soil water (e.g. Petrenko and Whitworth, 1999; Bittelli et al., 2003), as dissolved salts are excluded from the ice phase and remain in the unfrozen liquid phase. The supply of water toward the ice–liquid interface may eventually lead to the formation of ice lenses, and consequently to soil frost heaving. However, the magnitude of the water potential depression and thus the intensity of the water supply to the freezing front remains controversial (Black, 1995; Hohmann, 1997; Bronfenbrener and Bronfenbrener, 2010; Groenevelt and Grant, 2013). It seems that a reliable quantitative description of the complex processes accompanying the effect of cryosuction is yet to be developed, although some advances in this respect have been reported (e.g. Dall'Amico et al., 2011; Groenevelt and Grant, 2013; Tubini et al., 2017).

Increasingly, numerical models of varying complexity are used to simulate the thermal balance and water balance of soils exposed to freezing. Important aspects in soil freezing modeling are the highly non-linear nature of the energy balance equation during the phase transition and the coupling of thermal and mass balance equations describing energy and soil water fluxes. To handle the transformations between sensible and latent heat during freezing–thawing events, the majority of existing models employ the concept of apparent heat capacity (Harlan, 1973; Fuchs et al., 1978; Rankinen et al., 2004; Hansson et al., 2004; Dall'Amico et al., 2011; Endrizzi et al., 2014). As explained above, the main disadvantage of this approach is that the apparent heat capacity increases by several orders of magnitude at the freezing point, which complicates the numerical solution possibly causing numerical oscillations and convergence problems (e.g. Hansson et al., 2004; Dall'Amico et al., 2011).

A number of models include physically-based soil freeze–thaw routines of varying computational expense. For example: McKenzie et al. (2007) modified U.S. Geological Survey's SUTRA computer code to simulate fully saturated coupled pore water and energy transport in northern peatlands. Their freezing model is based on the apparent heat capacity concept, using empirical freezing functions to approximate the liquid water content versus freezing temperature relationship. They neglect the effects of cryosuction and freezing point depression due to dissolved salts in the porewater. Similar approach was used in the land-surface scheme of the Community Climate System Model (CLM) developed for simulations of permafrost dynamics, as described in Nicolsky et al. (2007). The Pan-Arctic Water Balance Model (PWBM) includes an approach similar to the CLM, modified by Rawlins et al. (2013). In another study, Bense et al. (2012) describe simulations with the generic finite element code FlexPDE designed to study the hydraulic regime of sub-permafrost aquifer systems. They assume that changes in water-content in freezing soil proceed from full water-saturation to full ice-saturation following the freezing curve approximated by a smoothed step function between 0 °C and –0.25 °C, and apply the apparent heat capacity concept to solve the heat flow equation. A comprehensive review of soil freezing models is given e.g. in Kurylyk and Watanabe (2013), who provide both historical and comparative study of basic theoretical principles and modeling approaches.

The objectives of the present study are: (1) to formulate a simplified, yet physically sound, approach for modeling water flow and energy transport in a variably-saturated partially frozen soil, applicable to episodic freezing conditions; (2) to develop a reliable non-iterative algorithm for solving the highly non-linear energy balance equation; (3) to verify the newly developed model against available analytical solutions of the energy balance equation; and (4) to provide examples of the model application to numerical simulations of freezing-thawing events.

2. Methods

2.1. Basic pore space partitioning relationships

The composition of soil is commonly expressed as a sum of volumetric fractions of individual soil constituents. We consider five constituents:

$$\varepsilon_m + \varepsilon_o + \varepsilon_i + \varepsilon_w + \varepsilon_a = 1 \tag{1}$$

where m stands for mineral particles, o for organic matter, i for ice, w for liquid water and a for air. The mineral particles and organic matter constitute the soil matrix. The soil pore volume is partitioned among three phases – ice, liquid water and air:

$$\varepsilon_i + \varepsilon_w + \varepsilon_a = \phi \tag{2}$$

where ϕ is the porosity (dimensionless). Further we assume that the soil matrix is rigid. This makes the description of phase changes during soil freezing easier, but, at the same time, it excludes some important phenomena accompanied by deformations of the soil matrix, namely the frost heaving.

Neglecting the presence of water vapor, the mass balance of soil water in the pore space requires that:

$$\rho_i \varepsilon_i + \rho_w \varepsilon_w = \rho_w \theta \tag{3}$$

where θ is the equivalent liquid water content (dimensionless), ρ_i is the density of ice (kg m^{-3}), and ρ_w is the density of liquid water (kg m^{-3}).

Under the assumption of rigid soil, it is useful to distinguish the water content at the liquid water saturation $\theta_s^{(w)}$ (equal to the saturated water content of unfrozen soil θ_s) and the equivalent liquid water content at the ice saturation $\theta_s^{(i)}$:

$$\theta_s^{(w)} = \theta_s = \phi \qquad \theta_s^{(i)} = \frac{\rho_i}{\rho_w}\phi \tag{4}$$

In the present version of our model, we assume that $\theta \le \theta_s^{(i)}$, so that the soil is always sufficiently unsaturated to allow for the ice expansion.

2.2. Soil thermal properties

Thermal properties of soil are characterized by the heat capacity and the soil thermal conductivity. The volumetric heat capacity of bulk soil can be evaluated based on the individual capacities of the soil constituents:

$$C = \begin{cases} \varepsilon_m c_m + \varepsilon_o c_o + \varepsilon_w c_w \text{ for unfrozen soil} \\ \varepsilon_m c_m + \varepsilon_o c_o + \varepsilon_i c_i \text{ for frozen soil} \end{cases} \tag{5}$$

where c_m, c_o, c_w and c_i are the volumetric heat capacities of mineral particles, organic matter, liquid water and ice (J m^{-3} K^{-1}). Note that the contribution of liquid water heat capacity in frozen soil is in the present version of our model neglected.

The soil thermal conductivity depends not only on the conductivities and fractions of individual soil constituents but also on their distribution within the soil. Each soil thus exhibits a specific relationship between the water content and the thermal conductivity. Moreover, when the water moves through the soil, the heat advection has to be taken into account. Therefor the apparent soil thermal conductivity function is defined as:

$$\lambda(\theta, q) = \lambda_e(\theta) + c_w d\,|q| \tag{6}$$

where $\lambda_e(\theta)$ is the thermal conductivity function (W m^{-1} K^{-1}) describing the $\lambda - \theta$ relationship for variably saturated conditions, d is the thermal dispersivity (m), which plays a similar role in the heat transport modeling as does the mechanical dispersivity in the solute transport modeling (de Marsily, 1986), and q is the soil water flux (m s^{-1}).

To approximate the thermal conductivity function, we use the approach of Côté and Konrad (2005):

$$\lambda_e^{(w)}(\theta) = \lambda_{dry} + (\lambda_{sat}^{(w)} - \lambda_{dry})\frac{\kappa\theta}{\theta_s^{(w)} + (\kappa - 1)\theta} \tag{7}$$

$$\lambda_{sat}^{(w)} = \lambda_m^{\varepsilon_m}\lambda_o^{\varepsilon_o}\lambda_w^{\phi} \qquad \lambda_{dry} = \frac{\chi}{10^{\eta\phi}} \tag{8}$$

where λ_{dry} and $\lambda_{sat}^{(w)}$ are the soil thermal conductivities at dry and water-saturated conditions (W m^{-1} K^{-1}), κ is an empirical parameter used to account for different textural soil classes (dimensionless), and χ (W m^{-1} K^{-1}) and η (dimensionless) are empirical parameters accounting for particle shape effects. Estimates of κ, χ and η for basic types of soils can be found in Côté and Konrad (2005).

Based on the data published by Côté and Konrad (2005), we suggest the following simplified form of the $\lambda_e(\theta)$ function for frozen soil conditions:

$$\lambda_e^{(i)}(\theta) = \lambda_{dry} + (\lambda_{sat}^{(i)} - \lambda_{dry})\frac{\theta}{\theta_s^{(i)}}$$
$$\lambda_{sat}^{(i)} = \lambda_m^{\varepsilon_m}\lambda_o^{\varepsilon_o}\lambda_i^{\phi} \tag{9}$$

An example of the parameterization of soil thermal conductivity function based on Côté and Konrad (2005) approach is given in Section 4.2 (Table 2).

2.3. Model assumptions

Following simplifying assumptions are made in the present version of our model: (1) Soil is rigid. No soil heaving due to ice expansion is allowed. (2) The freezing point depression of soil water is neglected. Soil water freezes and thaws at the temperature of 273.15 K. This assumption also means that the soil freezing function is approximated by a step function with infinite slope. Infinite slope can be applied because we do not use the concept of apparent heat capacity to formulate energy balance equation. (3) Liquid water in frozen soil is immobile and its amount is negligible. This assumption could be relaxed by including unfrozen residual water content in frozen soil, e.g. to improve the accuracy of frozen soil heat capacity estimation in soils with large residual water content (e.g. clayey soils). (4) Soil water potential depression at the freezing front, caused by interfacial forces and/or solute expulsion, is neglected. Consequently, the phenomenon of cryosuction is not accounted for.

The above set of assumptions clearly limits the applicability of our model. Nevertheless, we believe that there is a class of problems for which it might be beneficial to use a simplified solution, rather than more complex solutions requiring large amount of additional information − often loaded with considerable experimental and/or theoretical uncertainty.

2.4. Energy balance

In a soil system exposed to freezing–thawing conditions, a significant amount of energy is transferred between sensible and latent heat, which together contribute to the internal energy of the system. The internal energy can be expressed as:

$$U(\theta, T, \varepsilon_w) - U(\theta, T_0, 0) = L\varepsilon_w + C(\theta, T)(T - T_0) \tag{10}$$

where U is the internal energy of bulk soil (J m^{-3}), L is the product of the specific latent heat of fusion and liquid water density (J m^{-3}), ε_w is the liquid water content (dimensionless), T is the temperature (K), T_0 is the freezing point temperature (equal to 273.15 K). As we are interested only in changes of U and not in absolute values, it is convenient to assume that the internal energy of frozen soil at T_0 is equal to zero, or more precisely that $U(\theta,T_0,0) = 0$.

The volumetric heat capacity can be expressed as a linear function of equivalent liquid water content for temperatures above as well as below the freezing point (i.e., for fully unfrozen or fully frozen soil):

$$C(\theta, T) = \begin{cases} \varepsilon_m c_m + \varepsilon_o c_o + \theta c_w = C^+(\theta) & T > T_0 \\ \varepsilon_m c_m + \varepsilon_o c_o + \frac{\rho_w}{\rho_i}\theta c_i = C^-(\theta) & T < T_0 \end{cases} \tag{11}$$

The value of C at T_0 is not needed to evaluate U from Eq. (10), as the second term on the right-hand side of the equation is equal to zero for $T = T_0$. In fact, the heat capacity is undefined at the freezing point during phase transitions. However, we can assume that $C(\theta,T_0)$ is equal to either $C^+(\theta)$ or $C^-(\theta)$, depending on whether T_0 is approached from the above-freezing temperatures or below-freezing temperatures.

The local balance of internal energy in a soil system requires that:

$$\frac{\partial U}{\partial t} + \frac{\partial j_L}{\partial z} + \frac{\partial j_H}{\partial z} = -S_L - S_H \tag{12}$$

where j_L is the flux of latent heat (W m^{-2}), j_H is the flux of sensible heat (W m^{-2}), S_L and S_H are the sinks of latent and sensible heat due to the uptake of water by plant roots (W m^{-3}).

The latent and sensible heat fluxes are expressed as:

$$j_L = qL \qquad j_H = qc_w(T - T_0) - \lambda\frac{\partial T}{\partial z} \tag{13}$$

The latent and sensible heat sinks are specified as:

$$S_L = S_w L \qquad S_H = S_w c_w (T - T_0) \tag{14}$$

where S_w is the root water uptake intensity (s^{-1}).

After substituting (10), (13) and (14) into (12) and assuming that the equivalent liquid water content does not change with time when $T \le T_0$:

$$L\frac{\partial\varepsilon_w}{\partial t} + \frac{\partial CT}{\partial t} - c_w T_0\frac{\partial\theta}{\partial t} + c_w\frac{\partial qT}{\partial z} - c_w T_0\frac{\partial q}{\partial z} - \frac{\partial}{\partial z}\left(\lambda\frac{\partial T}{\partial z}\right) + L\frac{\partial q}{\partial z} =$$
$$-S_w L - S_w c_w T + S_w c_w T_0 \tag{15}$$

The terms involving T_0, i.e. the third and fifth term on the left-hand side together with the third term on the right-hand side, cancel out due to the equivalent liquid water balance. The equation then becomes:

$$L\frac{\partial\varepsilon_w}{\partial t} + \frac{\partial CT}{\partial t} + c_w\frac{\partial qT}{\partial z} - \frac{\partial}{\partial z}\left(\lambda\frac{\partial T}{\partial z}\right) + L\frac{\partial q}{\partial z} = -S_w L - S_w c_w T \tag{16}$$

The resulting energy balance equation can be decomposed into separate balance equations of sensible and latent heat:

$$\frac{\partial CT}{\partial t} + c_w\frac{\partial qT}{\partial z} - \frac{\partial}{\partial z}\left(\lambda\frac{\partial T}{\partial z}\right) + S_w c_w T = -Q \tag{17}$$

$$L\frac{\partial\varepsilon_w}{\partial t} + L\frac{\partial q}{\partial z} + S_w L = Q \tag{18}$$

where Q is the sink/source of internal energy (J m^{-3} s^{-1}) due to the phase transition. Sink in the sensible heat balance (17) represents source in the latent heat balance (18) and vice versa. The value of Q is positive for melting and negative for freezing. The magnitude of Q is determined by the rate of the phase change:

$$Q = -\frac{\rho_i}{\rho_w}L\frac{\partial\varepsilon_i}{\partial t} \tag{19}$$

Note that Eqs. (18) and (19) can also be interpreted as the mass balance equations for liquid and frozen water.

2.5. Soil water flow

Alternatively, the mass balance of soil water can be written in terms of the equivalent liquid water content:

$$\frac{\partial\theta}{\partial t} + \frac{\partial q}{\partial z} + S_w = 0 \tag{20}$$

Note that (20) can be obtained by combining (18), (19), and (3).

To describe the flow of soil water, the mass balance equation needs

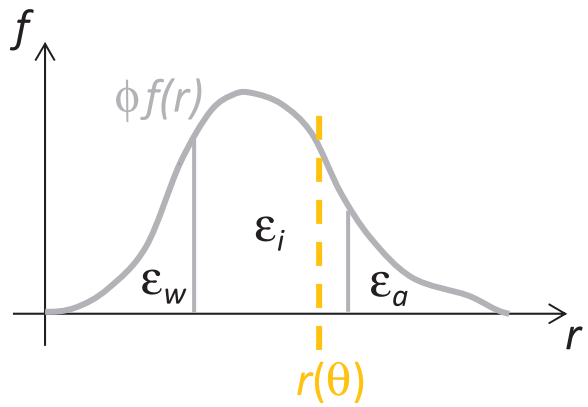

Fig. 1. Partitioning of pore space between liquid water, ice and air (ε_w, ε_i and ε_a are the volumetric fractions of liquid water, ice and air, $f(r)$ is the pore size distribution function, r is the pore radius, ϕ is the porosity, and θ is the equivalent liquid water content).

to be complemented with an appropriate momentum balance equation and corresponding constitutive relationships. In case of the unfrozen soil, this role is played by the Darcy-Buckingham equation and the functions representing soil hydraulic properties – the soil water retention function, $\theta(h)$, and the hydraulic conductivity function, $K(h)$:

$$q = K(h)\left(\frac{\partial h}{\partial z} + 1\right), \qquad \theta = \theta(h), \qquad K = K(h) \tag{21}$$

where h is the soil water pressure head (m). For freezing/thawing conditions, the situation becomes more complicated. It is common to assume that freezing of fully or partially saturated soil proceeds from water in large pores to progressively smaller ones (Fig. 1). Due to the freezing point depression, a small amount of water in frozen soil remains unfrozen even at temperatures well below 273.15 K. In our simplified modeling approach, we assume the amount and mobility of such water negligible. Consequently, the soil water flow is limited to unfrozen soil only. Under specific conditions, liquid water can also enter air-filled pores of partly saturated frozen soil (e.g. during rain-on-frozen-soil events). Such conditions are dealt with in our model by introducing a separate preferential flow domain (see the example problem presented in Section 4.2).

2.6. Numerical solution of energy balance

The numerical solution of the energy balance Eq. (17) has been implemented into the flow-and-transport code S1D (Vogel et al., 2010, 2011). The solution is based on the finite element method, which approximates the governing partial differential equation with a set of algebraic equations. The main challenge in solving this set of equations is associated with its strong nonlinearity during phase transition. The nonlinearity is a direct consequence of the abrupt change of internal energy as a function of temperature at the freezing point (Fig. 2).

In most, if not all, existing codes the nonlinear set of algebraic equations is solved iteratively, which makes the resulting algorithm computationally expensive and prone to problems with convergence. In what follows, we introduce a robust non-iterative solution.

We assume that the soil profile can be divided into three zones: (1) frozen soil, (2) freezing-thawing soil and (3) unfrozen soil. These zones are characterized by distinct internal energy regimes:

$$U = \begin{cases} C^-(T - T_0) & T < T_0 \\ L\varepsilon_w & T = T_0 \\ L\theta + C^+(T - T_0) & T > T_0 \end{cases} \tag{22}$$

An important aspect, which allows us to solve the energy balance equation by a non-iterative procedure, is that the freezing–thawing zone in the soil profile stays at the constant temperature T_0 during phase transition, i.e., until completely frozen ($\varepsilon_w = 0$) or completely unfrozen ($\varepsilon_w = \theta$).

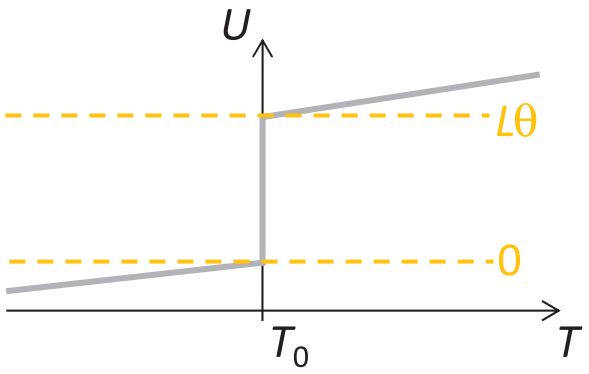

Fig. 2. Internal energy as a function of temperature (T_0 is the freezing point temperature, L is the product of the specific latent heat of fusion and liquid water density, and θ is the equivalent liquid water content).

The suggested numerical solution proceeds as follows. The application of the finite element method to solve the energy balance Eq. (17) results in a set of algebraic equations which needs to be solved for nodal temperatures at each time step. This set can be expressed as a tridiagonal matrix system. The n-th row of the system can be written as:

$$A_{1n}T_{n-1} + A_{2n}T_n + A_{3n}T_{n+1} = B_n - Q_n \tag{23}$$

where A and B are coefficients computed from the local soil thermal properties and soil water fluxes (i.e. from nodal values of C, c_w, λ, q and S_w) and Q_n is the nodal value of sink/source of internal energy due to the phase transition.

If a nodal value of internal energy U_n (calculated from Eq. (22)) drops below $L\theta$ by cooling of unfrozen soil or rises above zero by warming of frozen soil at any nodal point n (cf. Fig. 2), the coefficients of n-th row of the matrix system are stored and replaced by dummy values (denoted by asterisk) to force the matrix solver to produce $T_n = T_0$:

$$A^*_{1n} = 0,\ A^*_{2n} = 1,\ A^*_{3n} = 0,\ B^*_n = T_0,\ Q^*_n = 0 \tag{24}$$

This operation removes the phase transition singularity from the system. The resulting set of equations is linear and can be solved to yield the vector of unknown nodal temperatures T_n.

The original (previously stored and replaced) coefficients are then used to evaluate Q_n. After that, the values of Q_n are used to determine the changes of liquid water content ε_w caused by the phase transition at each nodal point of the freezing/thawing zone (cf. Eq. (19)):

$$\left(\frac{\Delta\varepsilon_w}{\Delta t}\right)_n = -\frac{\rho_i}{\rho_w}\left(\frac{\Delta\varepsilon_i}{\Delta t}\right)_n = \frac{Q_n}{L} \tag{25}$$

The resulting nodal values of liquid water content are then used to update the values of U_n (Eq. (22)) and the algorithm proceeds to the next time step.

3. Model verification

3.1. Freezing

The freezing branch of our algorithm was verified against the analytical solution developed for a semi-infinite water column (Neumann, 1860 (in Weber, 1901)). The initial temperature of the column was assumed to be +2 °C. The boundary temperature at the freezing end of the column was set equal to −5 °C. The solution deals with the freezing of pure water, therefore the soil porosity was set equal to 1. The model results are compared with the analytical solution in Fig. 3. The figure suggests a very good agreement between the two solutions.

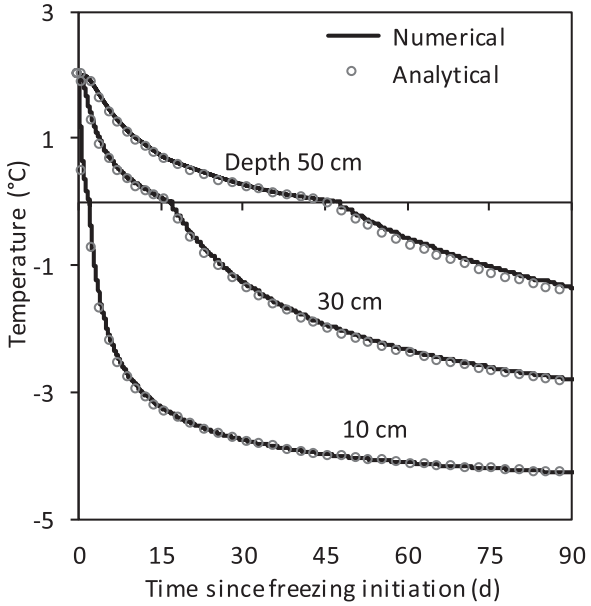

Fig. 3. Solution of the freezing case: temperature development at various depths as predicted by Neumann's analytical solution (in Weber, 1901) and S1D model.

3.2. Thawing

The penetration of thawing front into an initially frozen semi-infinite column of a saturated soil as a result of a sudden increase in surface temperature was solved analytically by Neumann (in Weber, 1901). His solution was used to verify the thawing branch of our algorithm. The initial temperature of −5 °C, porosity of 0.5 and boundary temperature of +5 °C were applied. The results of the numerical model are compared with the analytical solution in Fig. 4. The figure shows that the depth to thawing front predicted by the numerical model is in a very strong agreement with the analytical solution.

Table 1
Hydraulic parameters of the soil profile at the Liz catchment meadow site; The soil is conceptualized as a dual-continuum system represented by two flow domains: the soil matrix domain (SM) and the preferential flow domain (PF).

Domain	Depth (cm)	θ_r (–)	θ_s (–)	α (cm^{-1})	n (–)	K_s ($cm\ d^{-1}$)
SM	0–8	0.36	0.62	0.050	2.00	10
	8–100	0.15	0.40	0.024	1.25	1
	100–500	0.07	0.27	0.060	1.48	0.1
PF	0–100	0.05	0.43	0.11	2.00	1000
	100–500	0.05	0.43	0.11	2.00	0.1

θ_r and θ_s are the residual and saturated soil water contents, K_s is the saturated hydraulic conductivity, and α and n are empirical parameters determining the shape of the water retention and unsaturated hydraulic conductivity functions based on the parameterization of van Genuchten (1980). Parameter values were adopted from Votrubova et al. (2012).

4. Model application

4.1. Hypothetical freezing–thawing event

The following example problem deals with the numerical simulation of a hypothetical freezing–thawing event, occurring over a period of 24 days. The soil profile is homogeneous, 2 m deep, consisting of a sandy loam soil. The soil hydraulic and thermal properties correspond to a real soil (the second layer in Table 1).

The simulation starts with a uniform distribution of temperature in the soil profile. The initial temperature is set equal to +5 °C. At the time zero, the surface temperature drops down to −5 °C and then stays constant over the period of 10 days. After 10 days, the surface temperature increases back to +5 °C and remains constant over the rest of the simulated period.

As shown in Fig. 5, our model predicts a sharp freezing front separating the frozen soil above from the unfrozen soil below the front. During the initial 10-day period the freezing front advances to a depth of 30 cm. Next, the surface temperature increases above the freezing point, initiating the thawing phase of the event. During the thawing phase, two thawing fronts develop as the frozen soil warms up by heat conducted from the soil surface as well as from the deeper unfrozen part of the soil profile. The frozen soil between the two thawing fronts is quickly brought close to the freezing point. The thawing phase ends

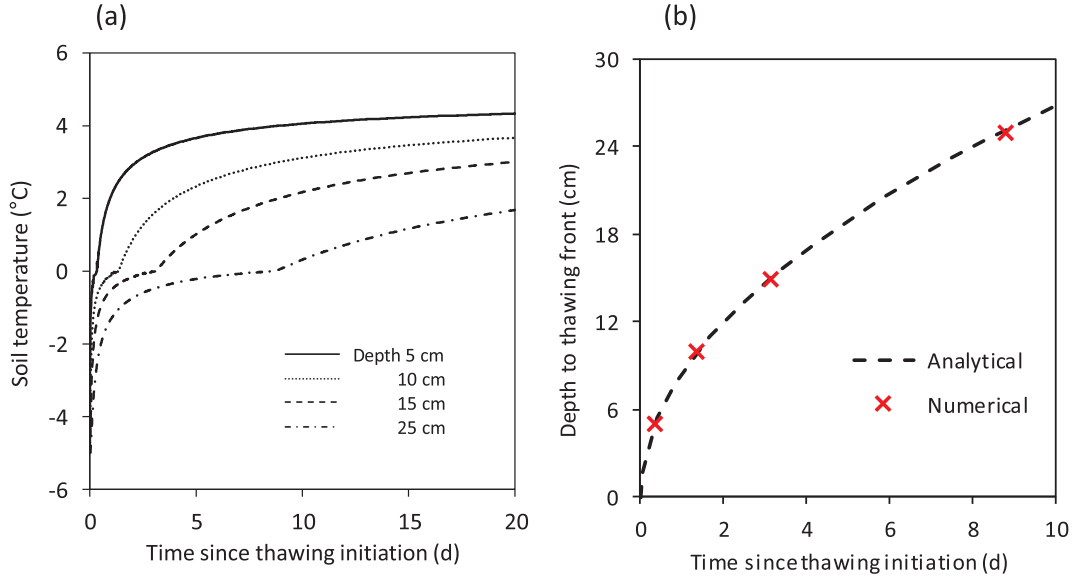

Fig. 4. Solution of the thawing case: (a) temperature development at various depths simulated by the S1D model; (b) the thawing front depth development predicted by Neumann's analytical solution (in Weber, 1901) and S1D model.

Table 2
Thermal parameters of the soil profile at the Liz catchment meadow site.

Domain	Depth (cm)	ε_m (–)	ε_o (–)	λ_{dry} (W m^{-1} K^{-1})	$\lambda_{sat}^{(w)}$ (W m^{-1} K^{-1})	κ (–)
SM	0–8	0.14	0.14	0.07	0.35	0.6
	8–100	0.58	0.02	0.25	1.42	1.9
	100–500	0.73	0	0.36	1.75	1.9
PF	0–8	0.43	0.14	0.23	1.26	1.9
	8–500	0.57	0	0.23	1.38	1.9

ε_m and ε_o are the volumetric fractions of of mineral and organic soil, λ_{dry} and $\lambda_{sat}^{(w)}$ are the soil thermal conductivities at dry and water-saturated conditions, κ is an empirical parameter used to account for different textural soil classes. The parametrization is based on the approach of Côté and Konrad (2005). Parameter values were adopted from Votrubova et al. (2012).

10 days after the surface temperature reversal, when the two thawing fronts meet.

4.2. Episodic soil freezing in a mountain catchment

The above described model was used to simulate winter thermal conditions at a meadow site of a mountain catchment. The site is situated in the Liz catchment – a small catchment belonging to the headwater area of the Otava river basin, located in the Bohemian Forest, Czech Republic. Hydraulic and thermal properties of the soil of interest (sandy loam developed on Paragneiss bedrock, classified as Eutric Cambisol) were adopted from Votrubova et al. (2012), while simplifying the description to three distinct layers as provided in Tables 1 and 2. The simulated soil profile was five meters deep, discretized with one-cm step.

The soil surface boundary condition was constructed using a simple snow cover model. Precipitation was considered liquid if the air temperature was not freezing. Snowmelt was approximated with a simple degree-day method. Melting occurred if the air temperature exceeded 0.1 °C. A sine wave was used to mimic the melt factor annual variation (between 0.05 and 0.25 cm °C^{-1} day^{-1}). The melt factor values were optimized to capture the snow disappearance time, deduced from the albedo observations.

The liquid precipitation and the snowmelt intensities were used to define the upper boundary condition of the soil water flow model (Fig. 6a). The bottom boundary condition was set according to the average specific discharge of the catchment (0.09 cm day^{-1}).

The soil temperature at the upper boundary was derived from the temperature measured 10 cm above the soil surface. Missing data for few days in December were substituted with the observations from previous and/or next days. For no-snow conditions, soil surface temperature was set equal to the air temperature measured 10 cm above ground. In case of snow cover, this air temperature was adjusted: the soil surface temperature was kept below zero (above-zero temperatures, observed above shallow snow cover, were not considered) and to account for the expected temperature attenuation due to the snow cover, temperature fluctuations below zero were reduced (in our case, dividing by two provided pleasing results). Constant temperature of 9 °C was set at the bottom of the simulated soil profile.

The S1D model was used in a dual-continuum mode to allow snowmelt water to infiltrate (passing the frozen soil-matrix layer). The preferential flow domain was assumed to be unaffected by water phase changes, i.e. remained fully conductive during freezing episodes.

Fig. 6b illustrates that the model can reproduce the soil freeze-thaw cycle reasonably well. The seasonal variation of the soil temperature near the soil surface is captured including timing of the soil thawing in spring (manifested by the soil temperature beginning to follow diurnal variations of the air temperature). In a detail view, the diurnal temperature variations in unfrozen soil are underestimated. This discrepancy is likely related to the inaccurate boundary condition, as the surface temperature daily amplitudes are probably bigger than those measured 10 cm above the surface. On the other hand, when the soil becomes frozen, the diurnal temperature variations are overestimated. This is probably due to the imperfect model representation of the soil surface layer thermal properties under frozen conditions: our assumption of negligible residual liquid water saturation may result in thermal conductivity overestimation in the highly rooted surface layer. Moreover, unlike the observation, the model indicates soil thawing in January. This could again be caused by the unrealistic boundary condition, i.e. by the near-surface air temperature being not an adequate proxy for the soil surface temperature.

5. Summary and conclusions

A new modeling approach was developed to facilitate the simulations of soil water flow and energy transport during sporadic freezing–thawing episodes, which are typical for the winter regime of humid temperate continental climate. The approach is based on an accurate non-iterative algorithm for solving highly non-linear energy balance equation during the phase transitions.

The suggested modeling approach abstracts from many complexities associated with the freezing phenomena in soils, yet preserves the principal physical mechanism of conserving the internal energy of the soil system during the phase transitions. When applied to simulate occasional freezing soil conditions, the model algorithm delivers the desired effect of slowing down the propagation of surface freezing temperatures into deeper soil horizons by converting water latent heat into sensible heat. The model also allows the evaluation of the extent and duration of frozen soil conditions – a crucial information for soil water flow modeling, as the frozen soil significantly reduces the soil hydraulic conductivity.

The new algorithm was successfully verified against analytical solutions for idealized freezing and thawing conditions. Two examples of the model application – under hypothetical and real field conditions –

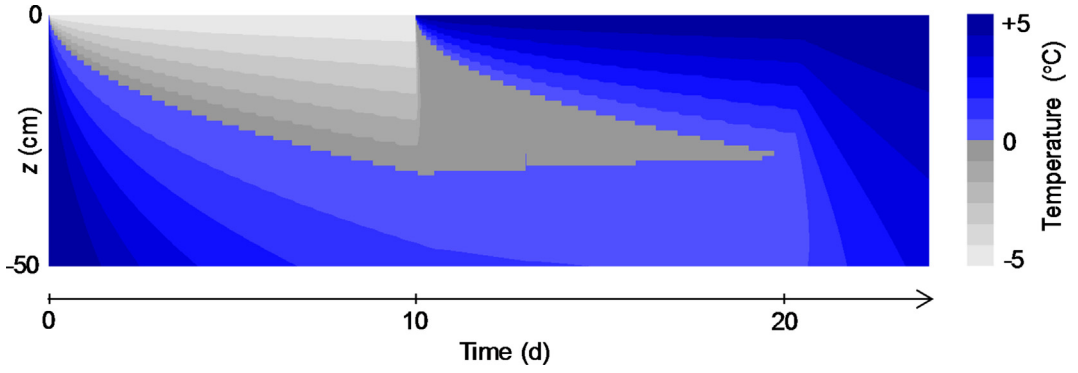

Fig. 5. Simulated development of the soil temperature profile during the freezing–thawing event (only the upper 50 cm layer of the 2 m deep soil profile is shown).

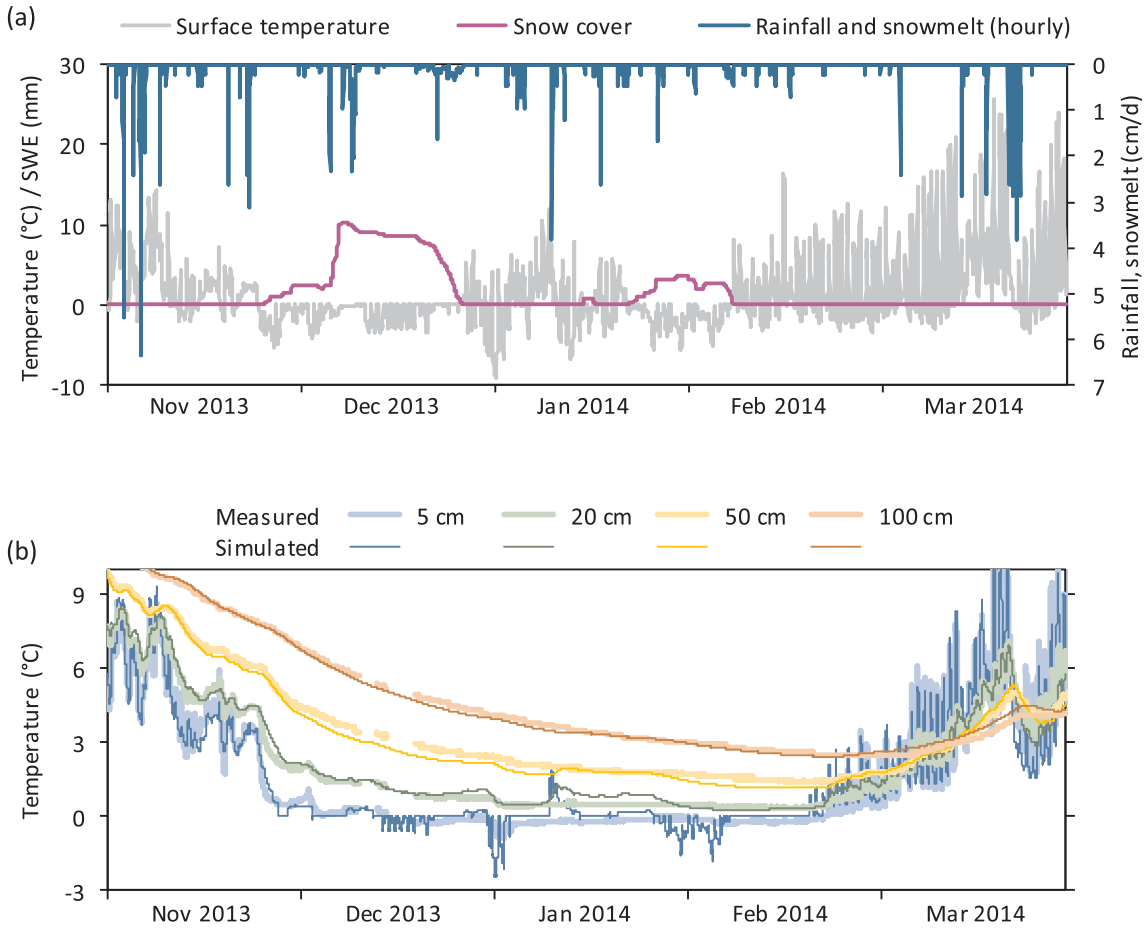

Fig. 6. Comparison of the observed and simulated soil temperatures at the meadow site of the Liz catchment during winter: (a) Upper boundary conditions (SWE stands for the Snow Water Equivalent); (b) Measured and simulated soil temperatures.

were given. The latter example shows that the model is capable of simulating transient freezing-thawing episodes and predicting the winter soil thermal regime at the site of interest.

Declaration of Competing Interest

The authors declare that they have no known competing financial interests or personal relationships that could have appeared to influence the work reported in this paper.

Acknowledgements

The research was funded by the Czech Science Foundation, projects no. 16-05665S and 17-00630J. Hydrometeorological data, utilized in Section 4.2, were available through the courtesy of the Institute of Hydrodynamics of the Czech Academy of Sciences.

References

Bense, V.F., Kooi, H., Ferguson, G., Read, T., 2012. Permafrost degradation as a control on hydrogeological regime shifts in a warming climate. J. Geophys. Res. 117, F03036. https://doi.org/10.1029/2011JF002143.

Bittelli, M., Flury, M., Campbell, G.S., 2003. A thermodielectric analyzer to measure the freezing and moisture characteristic of porous media. Water Resour. Res. 39 (2), 1041. https://doi.org/10.1029/2001WR000930.

Black, P.B., 1995. Applications of the Clapeyron equation to water and ice in porous media. Cold Regions Research & Engineering Laboratory, US Army Corps of Engineers.

Bronfenbrener, L., Bronfenbrener, R., 2010. Modeling frost heave in freezing soils. Cold Reg. Sci. Technol. 61, 43–64. https://doi.org/10.1016/j.coldregions.2009.12.007.

Cherkauer, K.A., Lettenmaier, D.P., 1999. Hydrologic effects of frozen soils in the upper Mississippi River basin. J. Geophys. Res. 104, 19 599–19 610. https://doi.org/10.1029/1999JD900337.

Coussy, O., 2005. Poromechanics of freezing materials. J. Mech. Phys. Solids 53 (8), 1689–1718. https://doi.org/10.1016/j.jmps.2005.04.001.

Côté, J., Konrad, J.-M., 2005. A generalized thermal conductivity model for soils and construction materials. Can. Geotech. J. 42 (2), 443–458. https://doi.org/10.1139/t04-106.

Dall'Amico, M., Endrizzi, S., Gruber, S., Rigon, R., 2011. A robust and energy-conserving model of freezing variably-saturated soil. The Cryosphere 5, 469–484. https://doi.org/10.5194/tc-5-469-2011.

de Marsily, G., 1986. Quantitative Hydrogeology. Academic Press, London.

Endrizzi, S., Gruber, S., Dall'Amico, M., Rigon, R., 2014. GEOtop 2.0: simulating the combined energy and water balance at and below the land surface accounting for soil freezing, snow cover and terrain effects. Geosci. Model Dev. 7, 2831–2857. https://doi.org/10.5194/gmd-7-2831-2014.

Fuchs, M., Campbell, G.S., Papendick, R.I., 1978. An analysis of sensible and latent heat flow in a partially frozen unsaturated soil. Soil Sci. Soc. Am. J. 42, 379–385. https://doi.org/10.2136/sssaj1978.03615995004200030001x.

Groenevelt, P.H., Grant, C.D., 2013. Heave and heaving pressure in freezing soils: a unifying theory. Vadose Zone J. 12. https://doi.org/10.2136/vzj2012.0051.

Hansson, K., Simunek, J., Mizoguchi, M., Lundin, L., van Genuchten, M., 2004. Water flow and heat transport in frozen soil numerical solution and freeze-thaw applications. Vadose Zone J. 3 (2), 693–704. https://doi.org/10.2136/vzj2004.0693.

Harlan, R., 1973. Analysis of coupled heat-fluid transport in partially frozen soil. Water Resour. Res. 9 (5), 1314–1323. https://doi.org/10.1029/WR009i005p01314.

Hohmann, M., 1997. Soil freezing – the concept of soil water potential. State of the art. Cold Reg. Sci. Technol. 25 (2), 101–110. https://doi.org/10.1016/S0165-232X(96)00019-5.

Kay, B.D., Groenevelt, P.H., 1974. On the interaction of water and heat transport in frozen and unfrozen soils: I. Basic theory; the vapor phase. Soil Sci. Soc. Am. J. 38, 395–400. https://doi.org/10.2136/sssaj1974.03615995003800030011x.

Koopmans, R.W.R., Miller, R.D., 1966. Soil freezing and soil water characteristic curves. Soil Sci. Soc. Am. J. 30, 680–685. https://doi.org/10.2136/sssaj1966.03615995003000060011x.

Kurylyk, B.L., Watanabe, K., 2013. The mathematical representation of freezing and thawing processes in variably-saturated, non-deformable soils. Adv. Water Resour. 60, 160–177. https://doi.org/10.1016/j.advwatres.2013.07.016.

Luo, L., Robock, A., Vinnikov, K.Y., et al., 2003. Effects of frozen soil on soil temperature, spring infiltration, and runoff: results from the PILPS 2 (d) experiment at Valdai,

Russia. J. Hydrometeorol. 4 (2), 334–351.
Ma, W., Zhang, Lianhai, Yang, Chengsong, 2015. Discussion of the applicability of the generalized Clausius-Clapeyron equation and the frozen fringe process. Earth-Sci. Rev. 142, 47–59. https://doi.org/10.1016/j.earscirev.2015.01.003.
McKenzie, J.M., Voss, C.I., Siegel, D.I., 2007. Groundwater flow with energy transport and water–ice phase change: numerical simulations, benchmarks, and application to freezing in peat bogs. Adv. Water Resour. 30, 966–983. https://doi.org/10.1016/j.advwatres.2006.08.008.
Miller, R.D., 1980. Freezing phenomena in soils. In: Hillel, D. (Ed.), Application of Soil Physics. Academic Press, pp. 254–299.
Mitchell, J., Beau, J., Webber, W., Strange, J.H., 2008. Nuclear magnetic resonance cryoporometry. Physics Reports 461 (1), 1–36. https://doi.org/10.1016/j.physrep.2008.02.001.
Nicolsky, D.J., Romanovsky, V.E., Alexeev, V.A., Lawrence, D.M., 2007. Improved modeling of permafrost dynamics in a GCM land-surface scheme. Geophys. Res. Lett. 34, L08501. https://doi.org/10.1029/2007GL029525.
Peppin, S.S.L., Style, R.W., 2013. The physics of frost heave and ice-lens growth. Vadose Zone J. 12. https://doi.org/10.2136/vzj2012.0049.
Petrenko, V.F., Whitworth, R.W., 1999. Physics of Ice. Oxford Univ. Press, New York.
Rankinen, K., Karvonen, T., Butterfield, D., 2004. A simple model for predicting soil temperature in snow-covered and seasonally frozen soil: model description and testing. Hydrol. Earth Syst. Sci. 8, 706–716. https://doi.org/10.5194/hess-8-706-2004.
Rawlins, M.A., Nicolsky, D.J., McDonald, K.C., Romanovsky, V.E., 2013. Simulating soil freeze/thaw dynamics with an improved pan-Arctic water balance model. J. Adv. Model. Earth Syst. 5. https://doi.org/10.1002/jame.20045.
Riseborough, D., Shiklomanov, N., Etzelmüller, B., Gruber, S., Marchenko, S., 2008. Recent advances in permafrost modelling. Permafrost Periglac. Process. 19, 137–156. https://doi.org/10.1002/ppp.615.
Strange, J.H., Rahman, M., Smith, E.G., 1993. Characterization of porous solids by NMR. Phys. Rev. Lett. 71 (21), 3589–3591. https://doi.org/10.1103/PhysRevLett. 71.3589.
Spaans, E.J.A., Baker, J.M., 1996. The soil freezing characteristic: its measurement and similarity to the soil moisture characteristic. Soil Sci. Soc. Am. J. 60, 13–19. https://doi.org/10.2136/sssaj1996.03615995006000010005x.
Taber, S., 1930. The mechanics of frost heaving. J. Geol. 38 (4), 303–317. https://doi.org/10.1086/623720.
Tubini, N., Serafin, F., Gruber, S., Casulli, V., Rigon, R., 2017. New insights in permafrost modelling. Geophys. Res. Abstr. 19 EGU2017-4870-1, EGU General Assembly 2017.
van Genuchten, M.Th., 1980. A closed form equation for predicting the hydraulic conductivity of unsaturated soils. Soil Sci. Soc. Am. J. 44, 892–898. https://doi.org/10.2136/sssaj1980.03615995004400050002x.
Vogel, T., Brezina, J., Dohnal, M., Dusek, J., 2010. Physical and numerical coupling in dual-continuum modeling of preferential flow. Vadose Zone J. 9, 260–267. https://doi.org/10.2136/vzj2009.0091.
Vogel, T., Dohnal, M., Votrubova, J., 2011. Modeling heat fluxes in macroporous soil under sparse young forest of temperate humid climate. J. Hydrol. 402, 367–376. https://doi.org/10.1016/j.jhydrol.2011.03.030.
Votrubova, J., Dohnal, M., Vogel, T., Tesar, M., 2012. On parameterization of heat conduction in coupled soil water and heat flow modelling. Soil Water Res. 7, 125–137. https://doi.org/10.17221/21/2012-SWR.
Weber, H., 1901. Die partiellen Differential-Gleinchugen der Mathematischen Physik, nach Riemann's Vorlesungen, t. II. Braunwschweig 118–122.